Investigations on the Directional Energy Decay Curves in Reverberation Rooms

Marco Berzborn and Michael Vorländer
Institute of Technical Acoustics, RWTH Aachen University, Aachen

Summary
The random incidence absorption coefficient is measured according to the international standard ISO-354 in a reverberation room with the prerequisite of the sound field in the room being diffuse. However, numerous studies showed high uncertainties in the method and a poor inter-laboratory reproducibility of the results. The assumption was drawn that these problems are in part caused by the violation of the diffuseness requirement. A robust metric for the diffuseness of sound fields in reverberation rooms is currently lacking, proving the characterization and calibration of reverberation rooms a complex problem.
To investigate the diffuseness of sound fields in reverberation rooms this study discusses the analysis of directional room impulse responses (DRIRs) and the spatial deviation of the corresponding directional energy decay curves. Applying spherical array processing methods, the DRIRs are calculated based on the decomposition of the sound field into plane waves composing the sound field. Multiple configurations of a reverberation room with varying degrees of sound field diffuseness are examined based on simulated spherical microphone array measurements.

PACS no. xx.xx.Nn, xx.xx.Nn

1. Introduction

Knowledge of the acoustic absorption properties of materials is crucial in the fields of building acoustics as well as room acoustic simulations. The random incidence absorption coefficient is measured according to the international standard ISO-354 [4] in a reverberation room with the prerequisite of the sound field in the room being diffuse. However, studies showed high uncertainties in the method and a poor inter-laboratory reproducibility of the results [3, 11]. The assumption arises that these problems are in part caused by a non-diffuse sound field [11]. A standardized robust metric for the characterization or calibration of reverberation rooms, however, is currently lacking [1].
Despite being a very fundamental concept, varying definitions for the diffuse sound field can be found in the literature [15]. The fundamental definition is that the diffuse sound field is isotropic – requiring the sound field to be composed of infinitely many sound waves from uncorrelated sources with directions of arrival (DOAs) uniformly distributed over a sphere [2, 5, 10]. The definition is also oftentimes used to express the diffuse sound as a superposition of uncorrelated plane waves with uniformly distributed DOAs [5, 10, 15]. One important consequence of diffuseness in rooms is an uniform sound pressure distribution within the room [2, 5, 6]
In this work we focus on the analysis of the isotropy of a sound field. Thiele [16] and Gover [2] discuss the distribution and spatial variation of energy incidence measured with a directional receiver in a room to study the isotropy of a sound field in steady state. This paper extends on this idea by further analyzing the spatial variation of the directional energy decay curves (DEDCs) which we calculate by applying the Schroeder integration [14] on directional room impulse responses (DRIRs).
Section 2 gives a brief introduction into the processing of DRIRs and the decomposition of the sound field, followed by the introduction of the DEDC. In Section 3 a simulation study of the DEDCs of a reverberation room in different configurations is presented. The results of this study are presented in Section 4, followed by the conclusions in Section 5.

2. Directional Room Impulse Response Analysis

Spherical microphone arrays (SMAs) allow for the capture of directional DRIRs retaining spatial information about the sound field in the room and there-

fore prove to be a viable tool in the analysis of sound field isotropy.

2.1. Directional Room Impulse Responses

A DRIR measured with an SMA can be written as a vector of room impulse responses (RIRs)

$$\mathbf{p}(t) = [p(t, \theta_1, \phi_1), \ldots, p(t, \theta_L, \phi_L)]^{\mathrm{T}}, \quad (1)$$

where θ_l and ϕ_l denote the elevation and azimuth angles of the l'th microphone and $(.)^{\mathrm{T}}$ denotes the transpose operator. Using the spherical harmonic (SH) transform[1] the DRIR may be expanded into a vector of SH coefficients $p_{nm}(t)$ of order n and degree m, respectively [17],

$$\mathbf{p_{nm}}(t) = [p_{0,0}(t), p_{-1,1}(t), \ldots, p_{N,N}(t)]^{T}, \quad (2)$$

with the a maximum SH order N. For the remainder of this paper, DRIRs will always be assumed to be coefficients in the SH domain. We now consider the sound field to be composed of a continuum of incoming plane waves and apply plane wave decomposition, yielding the plane wave amplitude density function [12]

$$a(t, \theta_q, \phi_q) = \frac{4\pi}{(N+1)^2} \mathbf{y}^{\mathrm{T}}(\theta_q, \phi_q) \mathbf{B}^{-1} \mathbf{p_{nm}}(t), \quad (3)$$

where

$$\mathbf{y}(\theta_q, \phi_q) = \left[Y_0^0(\theta_q, \phi_q), \ldots Y_N^N(\theta_q, \phi_q)\right]^{\mathrm{T}}, \quad (4)$$

is the steering vector of the array containing the real valued SH basis functions evaluated at the q'th steering direction defined by the angles $(\theta_q, \phi_)q$, respectively. $\mathbf{B}^{-1}$ is a diagonal matrix containing equalization filters for the elimination of the modal strength function of the array[2].
The plane wave decomposition may also be interpreted as a spatial filtering, yielding a new DRIR for every steering direction q, containing only contributions from the direction defined by (θ_q, ϕ_q).

2.2. Directional Energy Decay Curves

The energy decay curve (EDC) is a fundamental tool in the analysis of sound fields in rooms, providing information about the energy decay of a sound field in steady state in a room excited by broadband noise [8]. Schroeder [14] proposed the calculation of the EDC by an integration of the squared RIR. Analogously, we define the DEDC by performing the Schroeder integration on the amplitude density function from Eq. (3), yielding

$$\begin{aligned} d(t, \theta_q, \phi_q) &= \int_t^\infty |a(\tau, \theta_q, \phi_q)|^2 d\tau \\ &= e(\theta_q, \phi_q) - \int_0^t |a(\tau, \theta_q, \phi_q)|^2 d\tau, \end{aligned} \quad (5)$$

where $e(\theta_q, \phi_q)$ is the steady state energy arriving from a single discrete direction q calculated as

$$e(\theta_q, \phi_q) = \int_0^\infty |a(\tau, \theta_q, \phi_q)|^2 d\tau. \quad (6)$$

It has to be noted that this is only true for a causal system, requiring that $a(\tau, \theta_q, \phi_q) = 0$ for $\tau < 0$. An assumption that is usually made for RIRs [8].
Gover [2] and Thiele [16] used the mean of absolute spatial differences of the energy incidence from Q discrete directions

$$\sigma_e = \frac{1}{\langle e \rangle_s} \sum_{q=1}^{Q} |e(\theta_q, \phi_q) - \langle e \rangle_s|, \quad (7)$$

with the spatially averaged incident energy

$$\langle e \rangle_s = \frac{1}{L} \sum_{q=1}^{Q} e(\theta_q, \phi_q), \quad (8)$$

to discuss the isotropy – they refer to it as directional diffusion – of a sound field in a room. In a similar fashion we may extend Eq. (7) to study the spatial variation of the DEDC

$$\sigma_d(t) = \frac{1}{\langle d(t) \rangle_s} \sum_{q=1}^{Q} |d(t, \theta_q, \phi_q) - \langle d(t) \rangle_s|, \quad (9)$$

where $\langle d(t) \rangle_s$ is the spatial average of the DEDC at time instance t. Inserting Eq. (5) into Eq. (9) it may be seen that $\sigma_d(t = 0) = \sigma_e$. Thiele [16] and Gover [2] further included a normalization factor calculated as Eq. (7) for the case of a single plane wave, here referred to as $\sigma_{e,0}$. Analogously, we normalize Eq. (9)

$$\mu_d(t) = \frac{\sigma_d(t)}{\sigma_{e,0}}. \quad (10)$$

We propose the DEDC as a tool to analyze not only the isotropy of a sound field in a room in steady state, but to further study the isotropy of the energy decay of the sound field.

[1] We use real valued SH basis functions here following the Ambix phase convention [7] and N3D normalization as in [17].

[2] See Ref. [12] for further information.

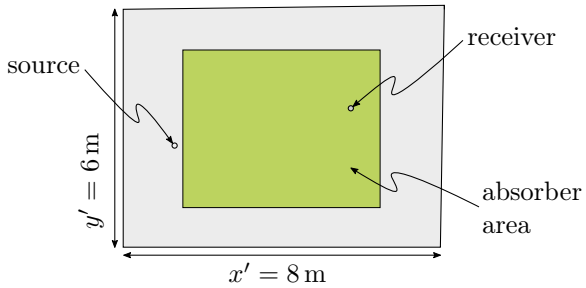

Figure 1. Top view of the simulated reverberation room with the receiver and source positions.

3. Simulation Study

A simulation study to examine the DEDCs of a hypothetical absorption coefficient measurement scenario in a reverberation room was conducted. The room model resembles an approximate cuboid with the dimensions $(x', y', z') = (8\,\mathrm{m}, 6\,\mathrm{m}, 4.5\,\mathrm{m})$, cf. Fig. 1. One corner was offset by 0.1 m to avoid simulation artifacts. The resulting volume of the room was $V = 220\,\mathrm{m}^3$. The source and receiver were positioned at $(x_s, y_s, z_s) = (1.3\,\mathrm{m}, 2\,\mathrm{m}, 1\,\mathrm{m})$ and $(x_r, y_r, z_r) = (5.75\,\mathrm{m}, 3.5\,\mathrm{m}, 2.75\,\mathrm{m})$, respectively, cf. Fig. 1. Both positions were chosen such that first order reflections do not share overlapping times of arrival.

The receiver was simulated as a virtual SMA in the SH domain with a maximum SH order $N = 10$. All DRIRs were simulated in the SH domain and already equalized for the modal strength function. The source was simulated as a point source with a perfectly omnidirectional directivity. Three different room configurations were simulated:

- C_1: An empty room, with almost rigid floor, and scattering elements on the sidewalls and ceiling.
- C_2: Same as C_1, but outfitted with an absorber with a surface area of $20\,\mathrm{m}^2$ on the floor.
- C_3: Almost rigid floor, sidewalls, and ceiling but outfitted with the same absorber configuration as in C_2.

Table I and Fig. 2 give a more detailed overview over the room configurations and corresponding materials.

Table I. Overview over the absorption and scattering coefficients α and s, respectively, for each simulated configuration.

Config	Floor	Ceiling	Walls	Absorber
C_1	α_r, s_r	α_s, s_s	α_s, s_s	α_r, s_r
C_2	α_r, s_r	α_s, s_s	α_s, s_s	α_a, s_a
C_3	α_r, s_r	α_r, s_r	α_r, s_r	α_a, s_a

All simulations were conducted using the room acoustic simulation software RAVEN [13] with an underlying hybrid simulation approach using the image source method up to second order and a ray-tracing algorithm for reflections of higher order. The simulation of DRIRs in the SH-domain is performed by simulating RIRs with receiver directivities corresponding to the SH basis functions. The DRIRs were simulated to allow for a valid calculation of the DEDCs to an energy decay of 40 dB. Further, the DEDCs were computed for a set of 500 azimuth and elevation angles determined using the equal area partitioning algorithm for spheres by Leopardi [9].

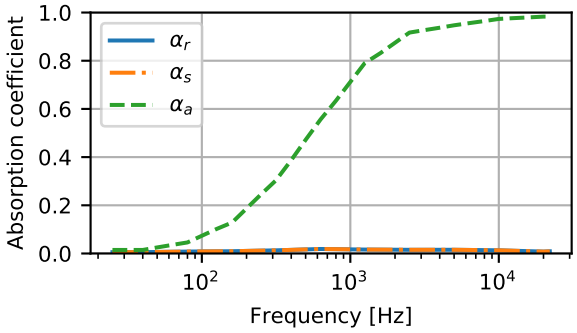

(a) Absorption coefficient

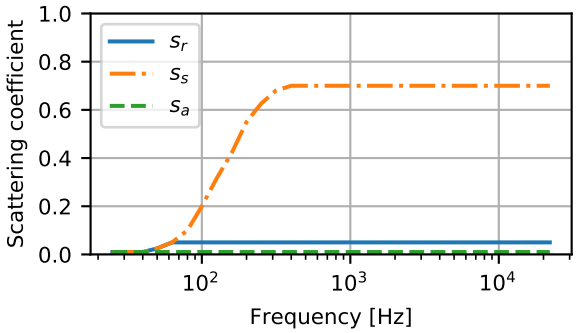

(b) Scattering coefficient

Figure 2. Absorption and scattering coefficients for the simulated materials.

4. Results

All results presented throughout the remainder of this paper are bandpass filtered to the 4 kHz octave band. The DEDCs were calculated according to Eq. (5) and truncated after a mean energy decay of 40 dB. Figs. 3 to 5 show the resulting DEDC for time instances t_μ corresponding to a mean energy decay of $0, 5, 10, 20, 30,$ and $40\,\mathrm{dB}$, respectively. The time instance t_0 represents the directional steady state energy incidence as calculated using Eq. (6). All DEDCs are normalized by the corresponding spatial mean $\langle d(t_\mu)\rangle_s$ and the color values are limited to a range of $(-5\,\mathrm{dB}, 5\,\mathrm{dB})$. The normalized mean of the absolute spatial differences defined in Eq. (10) can be studied in Fig. 6.

Comparing Figs. 3 to 5 at t_0 we expectedly find a

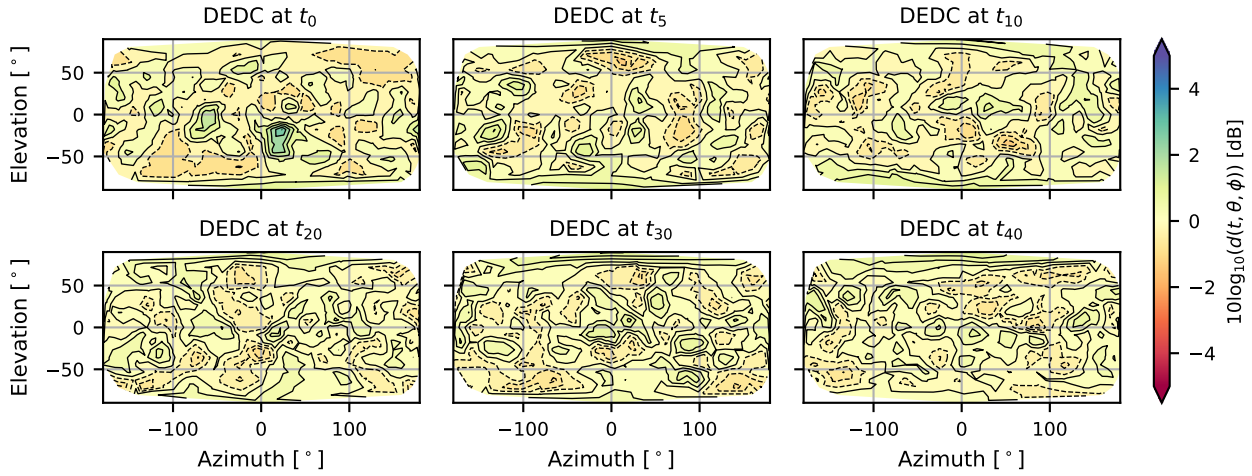

Figure 3. DEDC of configuration C_1 for time instances t_μ corresponding to a mean energy decay of $0, 5, 10, 20, 30$, and 40 dB, respectively. All curves are normalized by the corresponding spatial mean $\langle d(t_\mu)\rangle_s$.

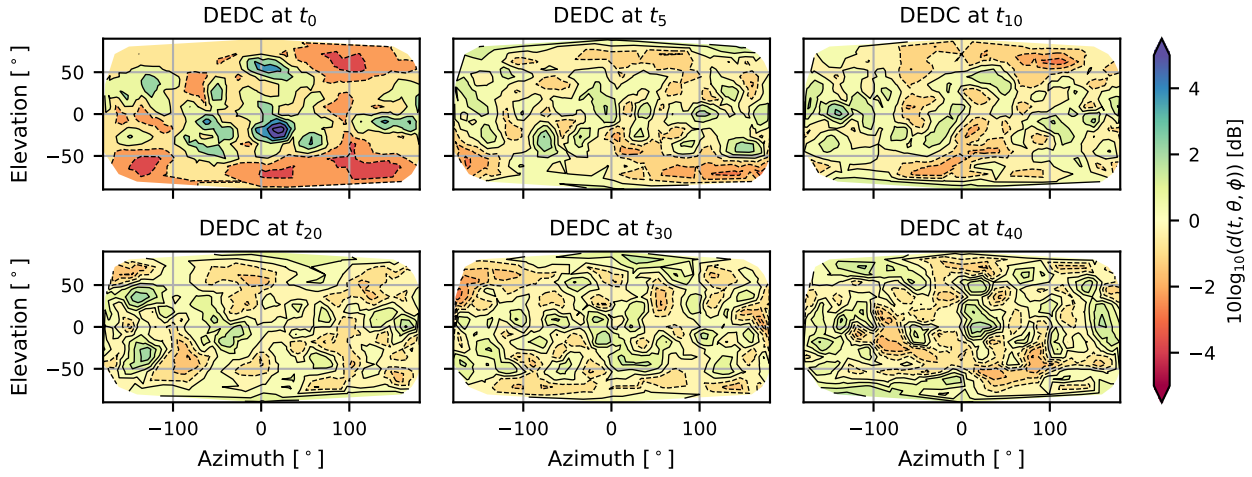

Figure 4. DEDC of configuration C_2 for time instances t_μ corresponding to a mean energy decay of $0, 5, 10, 20, 30$, and 40 dB, respectively. All curves are normalized by the corresponding spatial mean $\langle d(t_\mu)\rangle_s$.

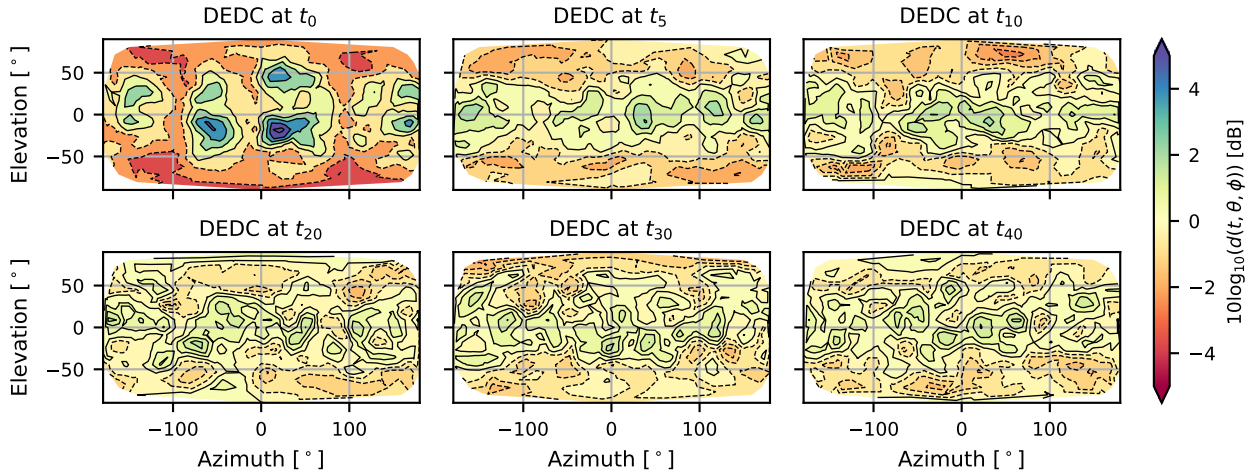

Figure 5. DEDC of configuration C_3 for time instances t_μ corresponding to a mean energy decay of $0, 5, 10, 20, 30$, and 40 dB, respectively. All curves are normalized by the corresponding spatial mean $\langle d(t_\mu)\rangle_s$.

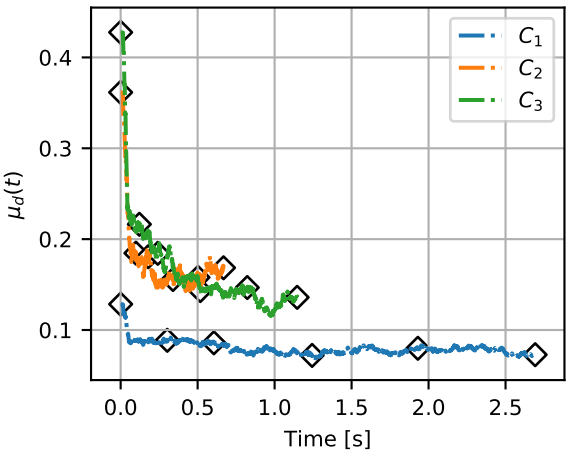

Figure 6. Mean spatial difference $\sigma_d(t)$ of the DEDC. All curves have been truncated to a maximum mean energy decay of 40 dB. The black markers indicate the time instance for an energy decay of $0, 5, 10, 20, 30$, and 40 dB, respectively.

maximum of incident energy at the DOA of the direct sound at $(\theta, \phi) = (20\,°, -20\,°)$. Strikingly, for the configurations including an absorber on the floor (cf. Figs. 4 and 5), this maximum shows to be more prominent. Further, additional maxima can be discriminated in at the DOAs of first order reflections, which are less pronounced for the room with scattering elements on the walls and the ceiling which cause more energy in the early reflections to be diffusely reflected rather than specularly. We can also observe a more uniform distribution of energy for configuration C_2, indicating a sound field with higher isotropy than in configuration C_3. This is also indicated by a lower mean of spatial differences in Fig. 6.

For configuration C_1 all DEDCs for time instances after the time of arrival of the direct sound share approximately the same dynamic range in their variation, cf. Figs. 3 and 6, indicating that the isotropy remains constant after subtracting energy corresponding to the direct sound. This decrease in the dynamic range in Fig. 4 is slower over time. Analogously, we observe a slower decrease in the spatial differences in Fig. 6. The increase in isotropy is expected as the number of reflections increases with time [8]. Interestingly, the DEDCs for configuration C_2 show a significantly slower energy decay in the xy-plane than in the xz-plane. Even though this effect decreases with time, it never fully vanishes. It is caused by specularly reflected waves traveling in the xy-plane without being deflected into the absorber (cf. Ref. [8]), eventually resulting in two-dimensional wave field rather than a three-dimensional one. Clearly, this phenomenon contradicts the definition of an isotropic sound field and might be interpreted as a systematic defect in the isotropy of the sound field. Despite this systematic defect, the spatial variation of the DEDCs at t_{20}, t_{30}, and t_{40} for configuration C_3 is smaller than for C_2, which is simply caused by higher amplitude variations. However, Fig. 6 indicates a faster increase of isotropy over time for C_2, which may also be identified in Figs. 4 and 5 for time instances t_5 and t_{10}.

5. Conclusions

In this paper we introduced the directional decay curve based on directional room impulse responses as a tool for the analysis of the isotropy of sound fields in rooms. A simulation study was conducted showing how studying variation of the directional decay curve applies to characterizing sound fields in reverberation rooms. It was further shown that the directional decay curve may provide a useful tool to identify systematic defects in the isotropy of a sound field.

Acknowledgement

The Authors would like to thank Lukas Aspöck for the fruitful discussions.
Work presented here was funded by the Deutsche Forschungsgemeinschaft under Grant VO 600 41-1.

References

[1] David T. Bradley et al. “Effect of Boundary Diffusers in a Reverberation Chamber: Standardized Diffuse Field Quantifiers”. In: *The Journal of the Acoustical Society of America* 135 (2014), pp. 1898–1906.

[2] Bradford N. Gover, James G. Ryan, and Michael R. Stinson. “Microphone Array Measurement System for Analysis of Directional and Spatial Variations of Sound Fields.” In: *The Journal of the Acoustical Society of America* 112.5 (2002), pp. 1980–1991.

[3] R. E. Halliwell. “Inter-laboratory Variability of Sound Absorption Measurement”. en. In: *The Journal of the Acoustical Society of America* 73.3 (Mar. 1983), pp. 880–886.

[4] International Organization for Standardization. *ISO 354:2003 - Measurement of Sound Absorption in a Reverberation Room*. 2003.

[5] Finn Jacobsen and Thibaut Roisin. “The Coherence of Reverberant Sound Fields.” In: *The Journal of the Acoustical Society of America* 108.1 (2000), pp. 204–210.

[6] Cheol-Ho Jeong. “Diffuse Sound Field: Challenges and Misconceptions”. In: *Proceedings of 45th International Congress and Exposition on Noise Control Engineering*. Hamburg, 2016, pp. 1015–1021.

[7] Matthias Kronlachner and Franz Zotter. “Spatial Transformations for the Enhancement of Ambisonic Recordings”. In: *Proceedings of the 2nd International Conference on Spatial Audio, Erlangen*. 2014.

[8] Heinrich Kuttruff. *Room Acoustics*. 4th Ed. Taylor & Francis, 2009.

[9] Paul Leopardi. "A Partition of the Unit Sphere into Regions of Equal Area and Small Diameter". In: *Electronic Transactions on Numerical Analysis* 25.12 (2006), pp. 309–327.

[10] Melanie Nolan et al. "A Wavenumber Approach to Characterizing the Diffuse Field Conditions in Reverberation Rooms". In: *Proceedings of the 22nd International Congress on Acoustics*. Buenos Aires, Sept. 2016.

[11] Mélanie Nolan et al. "The Use of a Reference Absorber for Absorption Measurements in a Reverberation Chamber". In: *Proceedings of Forum Acusticum*. Krakow, 2014.

[12] Boaz Rafaely. "Plane Wave Decomposition of the Sound Field on a Sphere by Spherical Convolution". In: *The Journal of the Acoustical Society of America* 116.4 (2004), pp. 2149–2157.

[13] Dirk Schröder. "Physically Based Real-Time Auralization of Interactive Virtual Environments". Dissertation. Institute of Technical Acoustics, RWTH Aachen University, 2011.

[14] M. R. Schroeder. "New Method of Measuring Reverberation Time". In: *The Journal of the Acoustical Society of America* 37.6 (1965), pp. 1187–1187.

[15] T. J. Schultz. "Diffusion in Reverberation Rooms". In: *Journal of Sound and Vibration* 16.1 (1971), pp. 17–28.

[16] Rolf Thiele. "Richtungsverteilung Und Zeitfolge Der Schallrückwürfe in Räumen". In: *Acta Acustica united with Acustica* 3.4 (1953), pp. 291–302.

[17] Earl G. Williams. *Fourier Acoustics*. Academic Press, 1999.